Aerospace Science and Technology 55 (2016) 332–343

Contents lists available at ScienceDirect

Aerospace Science and Technology

www.elsevier.com/locate/aescte

Fuselage aerodynamic prediction methods

Fabrizio Nicolosi, Pierluigi Della Vecchia *, Danilo Ciliberti, Vincenzo Cusati

University of Naples "Federico II", Via Claudio 21, 80125 Naples, Italy

ARTICLE INFO

Article history:
Received 19 January 2016
Received in revised form 9 June 2016
Accepted 10 June 2016
Available online 16 June 2016

Keywords:
Aircraft design
Fuselage aerodynamics
Turboprop aircraft

ABSTRACT

A reliable estimation of the aerodynamics of the fuselage of an airplane is crucial in order to carry out a well-designed aircraft. About 30% of an aircraft zero-lift drag source is due to the fuselage. Its aerodynamic instability is impacting wing and horizontal tail design, as well as aircraft directional stability characteristics. This paper proposes methods, developed through CFD analyses, to estimate fuselage aerodynamic drag, pitching, and yawing moment coefficients. These methods are focused on the regional turboprop aircraft category. Given the fuselage geometry, several charts allow to evaluate its aerodynamic characteristics. Numerical test cases are shown on several fuselage geometries and a comparison with typical semi-empirical methods is presented.

1. Introduction

This paper presents new preliminary design methodologies to estimate the aerodynamic coefficients of transport aircraft fuselage. Methods have been developed by numerical aerodynamic analyses performed with STAR-CCM+® (Ref. [1]) and they have been focused on the estimation of aerodynamic drag, pitching moment, and yawing moment coefficients. A similar approach to develop a preliminary design method has already been carried out by the authors, which have deeply investigated the aerodynamics of the vertical tailplane and the aerodynamic interference among airplane components asymmetric conditions [2,3]. The result of these studies is a methodology which effectiveness is not limited to the turboprop air transport category, but it has also been exploited for the preliminary design of a new general aviation commuter aircraft [4,5]. Fuselage design is particularly critical for commuter aircraft and general aviation categories, concerning drag and static stability contribution, which can strongly affects the tailplane sizing, as outlined in Ref. [5]. Especially for general aviation category, the choice of fuselage tailcone angle is also critical to achieve the best vertical location of the horizontal tailplane [4–6]. CFD calculations performed on bodies and wing-body combinations show in general a very good agreement respect to experimental data obtained through wind-tunnel tests performed by the authors [6].

The aerodynamic design of the fuselage of a regional transport aircraft is a crucial item in airplane preliminary design. About 30% of zero lift drag is due to the fuselage [7]. Aircraft cruise performance, such as maximum flight speed or fuel consumption, are mainly dependent from the zero-lift drag coefficient and they could be improved with a more accurate aerodynamic design. Moreover aircraft longitudinal and directional stability characteristics are strictly related to the fuselage contribution, thus an accurate estimation of the latter could lead to a better tailplane design and aircraft stability characteristics.

In a previous article [7], the authors have also highlighted the importance of a good aerodynamic design of the wing–fuselage junction or "karman" as usually defined for high mounted wing regional transport aircraft.

Aircraft preliminary design usually relies on semi-empirical methodologies, based on heritage aircraft geometries and wind tunnel tests mainly conducted by NACA [8–12]. Semi-empirical methods consider the drag coefficient as the sum of different contributions that can be evaluated by relations obtained from wind tunnel test data, most of which are collected in the USAF DATCOM database [13,14]. The total drag coefficient of an aircraft can be expressed as the sum of the zero-lift drag coefficient and the drag-due-to-lift coefficient. This assumption is valid when the approximation of a parabolic drag polar is used in order to estimate the drag coefficient for low incidence, such as cruise and climb, that is until the lift coefficient becomes greater than 1. The zero-lift drag coefficient is also known as parasite drag coefficient and it includes skin friction (function of wetted area), windshield angle ψ, upsweep angle θ, and base drag contributions [13–15].

Moreover, semi-empirical methods are also used to predict the moment coefficients. One of the most used is the *strip-method* where the fuselage is divided into strips, each of which gives a

* Corresponding author.
E-mail addresses: fabrizio.nicolosi@unina.it (F. Nicolosi), pierluigi.dellavecchia@unina.it (P. Della Vecchia), danilo.ciliberti@unina.it (D. Ciliberti), vincenzo.cusati@gmail.com (V. Cusati).

http://dx.doi.org/10.1016/j.ast.2016.06.012
1270-9638/

Nomenclature

b	= wing span	L	= fuselage length
c	= fuselage cabin	mac	= mean aerodynamic chord
C_D	= drag coefficient	n	= fuselage nose
C_M	= pitching moment coefficient	S_{front}	= fuselage frontal area
C_{M0}	= zero α pitching moment coefficient	S_{wet}	= wetted area
$C_{M\alpha}$	= pitching moment coefficient derivative	S_w	= wing area
d_f	= fuselage maximum diameter	t	= fuselage tailcone
f, fus	= fuselage	α	= angle of attack
fp	= flat plate	θ	= tailcone upsweep angle
FR	= fineness ratio	ψ	= windshield angle
K	= aerodynamic interference factor		

contribution to the pitching moment according to its distance from the wing [16].

In this paper, the approach presented by the authors in Ref. [17] has been expanded. From a reference fuselage layout (see Fig. 1), the nose, cabin (constant fuselage diameter), and tailcone geometry have been parametrically changed. Then, the aerodynamic drag, the pitching moment at zero incidence, the longitudinal static stability derivative, and the yawing moment coefficients C_D, C_{M0}, $C_{M\alpha}$, and $C_{N\beta}$ respectively, have been evaluated by numerical analyses (Reynolds-averaged Navier–Stokes – RANS – equations). Fuselage lift coefficient is not presented, due to the very low relevance in isolated fuselage geometry design. However, fuselage effect on aircraft lift coefficient has to be carefully evaluated and taken into account during the design phase, especially in the wing integration. Aerodynamic effects of each component (nose, cabin, tailcone) have been directly obtained from the CFD aerodynamic solver, separating the forces and moments contributions of each fuselage part.

Researchers at University of Naples have been working on the development of design techniques for light and general aviation aircraft since 1996. The aerodynamic calculations performed by the authors on general aviation aircraft configurations, also concerning the fuselage contribution to aircraft lift, drag, and stability, which have also been validated through flight test data, reported on specific articles [18,19]. In particular, the numerical estimation of the neutral stability point (which is strongly affected by fuselage contribution) through low-fidelity method and through CFD analyses for P2006T aircraft has shown very good agreement respect to wind-tunnel test results and flight test data collected and described in Refs. [18,19].

Section 2 shows the fuselage geometries involved in this paper, Section 4 describes the drag coefficient prediction method and some applications, Section 5 and 6 illustrate the pitching and yawing moment prediction method respectively. Finally conclusions are addressed.

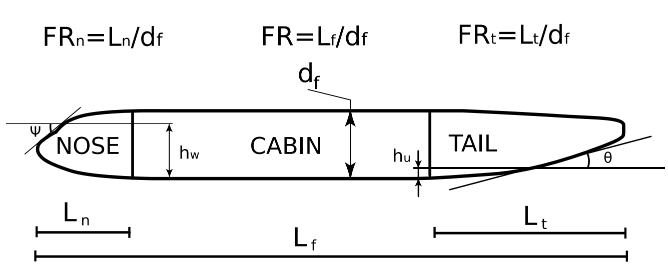

Fig. 1. Main fuselage geometrical parameters.

2. Fuselage geometries

A modular model of an 80-seats fuselage of a generic regional turboprop aircraft, which leads to a full scale fuselage length of about 30 m and diameter of 3.4 m, has been considered as reference layout. This geometry has been divided into three main components: nose, cabin, and tailcone (see Fig. 1). For each component, main geometrical parameters have been defined as shown in Fig. 1 and summarized in Table 1. The ratio of the fuselage length and diameter is the fineness ratio FR, whereas the ratio between the nose length and diameter, and tailcone length and diameter, are respectively the fineness ratio of the nose FR_n and of the tail FR_t. In order to define the windshield (ψ) and upsweep (θ) angles, the h_w and h_u parameters have been introduced. The first locates the height of the intersection point between the horizontal line and the tangent to nose contour. The latter locates the height of the intersection point between the horizontal line and the tangent to tail contour. Both are defined in Table 1.

Starting from the reference fuselage, many different geometries have been generated and parametric analyses have been performed. In particular, when the parametric investigation is performed on the nose, the cabin and the tailcone are those of the reference layout. Similarly, when the cabin length is changed, the nose and the tailcone are those of the reference layout. Of course, when the tailcone is varied, the nose and the cabin are those of the reference layout. Fig. 2 shows how the geometries have been built in a parametric way.

3. Numerical model

The numerical simulations have been performed with STAR-CCM+ on the University's grid computing infrastructure SCoPE [20] to simulate many configurations in a short amount of time. The numerical domain is externally bounded by a cuboid block, representing the farfield, and internally bounded by the fuselage surface, which is located on the block's longitudinal symmetry plane, at one third of the block length from the inlet boundary. Flow and energy are modeled by the STAR-CCM+ coupled flow model. The convergence rate does not deteriorate as the mesh is refined [1]. The flow is fully turbulent, modeled by the Spalart-Allmaras (SA) equation [21], which has proved to be reliable for external aerodynamics [22,23]. Mesh quality has been evaluated

Table 1
Definition of geometrical parameters.

L_f	d_f	L_n	L_c	L_t	FR	FR_n	FR_t	h_w/d_f	h_u/d_f	ψ	θ
30 m	3.4 m	5.7 m	13 m	11.3 m	8.7	1.6	2.8	0.75	0.26	40°	14°